Suzaku/XIS background report

H. Katayama*, M. Namiki, E. D. Miller, K. Hayashida, H. Yamaguchi, T.G. Tsuru, and the XIS team

December 16, 2005

ver 0.0 2005/09/21
ver 0.1 2005/12/10
ver 0.2 2005/12/14
ver 0.3 2005/12/16

Abstract

We present an initial report on the background of the X-ray Imaging Spectrometers (XISs) onboard Suzaku.

1 Internal background

1.1 Internal background while the XIS door was closed

In an initial operation phase for which the XIS door was closed, we could take the spectrum of an internal background. Unfortunately, most of the data took in the initial operations were reached to the telemetry limit. So, we need some corrections to the effective exposure time against the telemetry saturation, for which software tools have not been established yet. However, we can examine the internal background spectra without this correction.

Figure 1 shows the spectrum of internal background taken while the XIS door was closed. As a calibration source is attached to the XIS door[1], the intensity of the calibration source is stronger than other lines. Except for emission lines from the calibration source (MnKα:5.90 keV, and MnKβ:6.49 keV), and escape lines (MnKα escape:4.05 keV, MnKβ escape:4.64 keV, and Si:1.74 keV), we can see the fluorescent lines from camera body (Al:1.49 keV, AuMα:2.12 keV, NiKα:7.48 keV, NiKβ:8.27 keV, and AuLα-1:9.71 keV).

1.2 Night earth (Dark earth) observation

After the XIS door open (Aug. 12–13), we are collecting the data while Suzaku was looking at the dark side of the earth (night earth). We selected night earth event during the following condition,

```
ELV<-10 && DYE_ELV>100 && SAA.eq.0 && T_SAA > 256.
```

Figure 2 shows the background spectrum of XISs. These are night earth data taken from Aug. 2005 to Nov. 2005. The total exposure time is about 200 ks. The count rate of the internal background in 0.5–10.0 keV and emission lines are listed in Table 1.

The intensity of the MnKα and MnKβ lines of XIS0 are stronger than other three sensors. These lines are considered to be scattered X-rays from the calibration source on the door or on the corner. Figure 3 shows the XIS0 image of 5.7–6.0 keV. The intensity of these lines seems to be stronger in the lower half of the image. We will continue to examine the spatial distribution of these lines scattered from calibration sources.

1.3 COR Effects

As well as ASCA/SIS[1], the XIS background rate have a dependency on the magnetic cut-off rigidity (COR). We investigated the background count rate dependency on COR.

Figures 4 and 5 shows the internal background spectrum taken from the different COR region. The count rate of the background increases with decreasing COR. Figures 6 and 7 show a plot of count rate for different energy bands as a function of COR. The dependency on COR is similar in all energy bands. The background count rate of 4–6 GeV/c is about twice as high as that of 12–14 GeV/c.

*E-mail: katayama.haruyoshi@jaxa.jp

[1] There are two kinds of calibration sources (^{55}Fe) in XIS; one is attached on the XIS door and was available only when the door was closed, and the other is attached on the inner wall of the XIS bonnet and always available. The former is much stronger than the latter and irradiates the whole CCD area. The latter is equipped with a collimator and irradiates only at the two corners of each CCD.

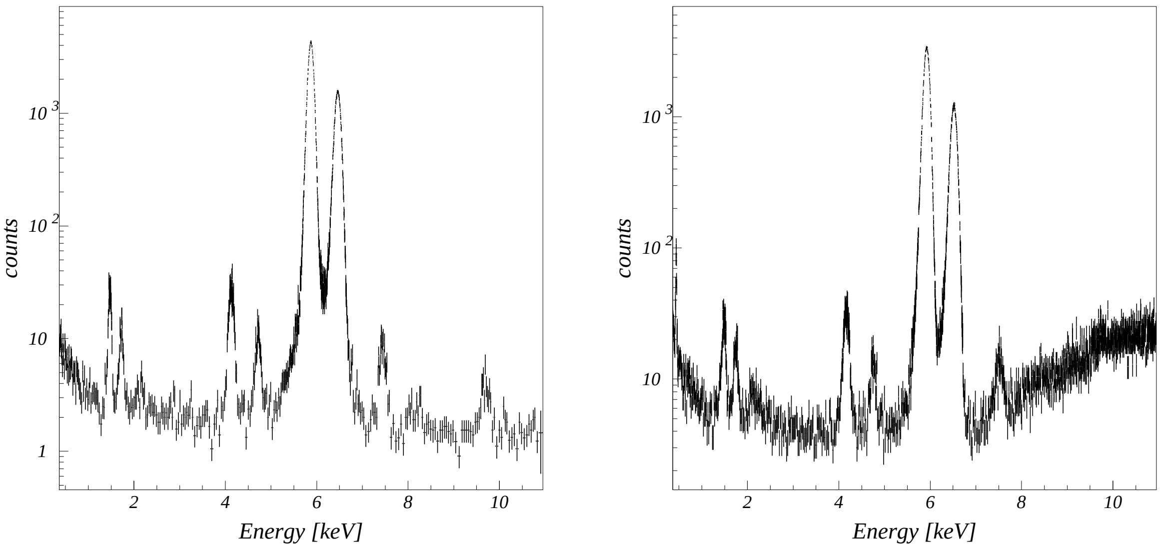

Figure 1: Internal background spectrum of the XIS taken while the XIS door was closed. The spectrum of the XIS-FI (XIS0) is left and that of the XIS-BI (XIS1) is right. MnKα, MnKβ lines from the calibration source attached inside the door are stronger than other components. Note that most of the X-rays from the calibration source on the XIS door does not enter the CCD after the door was opened.

Table 1: Count rate of the XIS Background[3].

Line	Energy keV	XIS0 10^{-9} ct/s/pix	XIS1 10^{-9} ct/s/pix	XIS2 10^{-9} ct/s/pix	XIS3 10^{-9} ct/s/pix
Total counts	0.5–10	75.3±0.4	224.7±6.7	81.9±4.0	87.7±4.2
Al Kα	1.486	1.98±0.23	3.01±0.51	$1.50^{+0.31}_{-0.28}$	$1.57^{+0.25}_{-0.23}$
Si Kα	1.740	$0.299^{+0.2080}_{-0.2074}$	2.21±0.45	0.0644($<$ 0.282)	$0.543^{+0.212}_{-0.213}$
Au Mα	2.1229	0.581±0.234	$1.13^{+0.280}_{-0.291}$	$0.359^{+0.211}_{-0.212}$	$6.69^{+2.91}_{-2.90}$
Mn Kα	5.898	$8.35^{+0.36}_{-0.34}$	0.648±0.289	$0.299^{+0.209}_{-0.2086}$	$0.394^{+0.181}_{-0.18}$
Mn Kβ	6.490	$1.03^{+0.22}_{-0.216}$	0.294($<$ 0.649)	0.00($<$ 0.111)	$0.428^{+0.225}_{-0.226}$
Ni Kα	7.470	7.20±0.31	6.24±0.53	$3.78^{+0.26}_{-0.25}$	$7.13^{+0.36}_{-0.37}$
Ni Kβ	8.265	0.583±0.183	$1.15^{+0.5}_{-0.489}$	0.622±0.206	$0.983^{+0.247}_{-0.249}$
Au Lα	9.671	$3.52^{+0.27}_{-0.28}$	$3.28^{+1.16}_{-0.99}$	$1.88^{+0.31}_{-0.28}$	$3.54^{+0.36}_{-0.35}$
Au Lβ	11.514	$2.25^{+0.73}_{-0.59}$	2.91±1.29	$0.752^{+0.428}_{-0.304}$	$2.67^{+0.61}_{-0.53}$

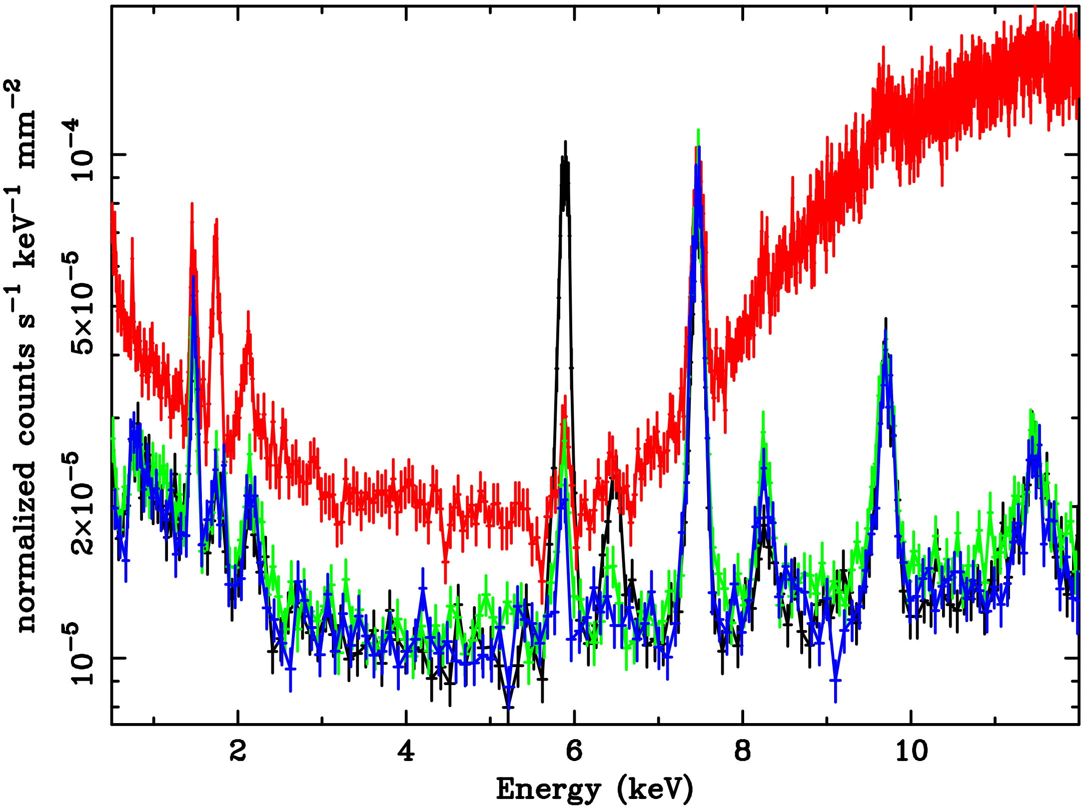

Figure 2: Comparison of the internal background of four XISs (XIS0:black, XIS1:red, XIS2:green, and XIS3:blue). Two cal sources on the corner are removed

Figure 3: XIS0 image of 5.7–6.0 keV (night earth data 200ks).[3]

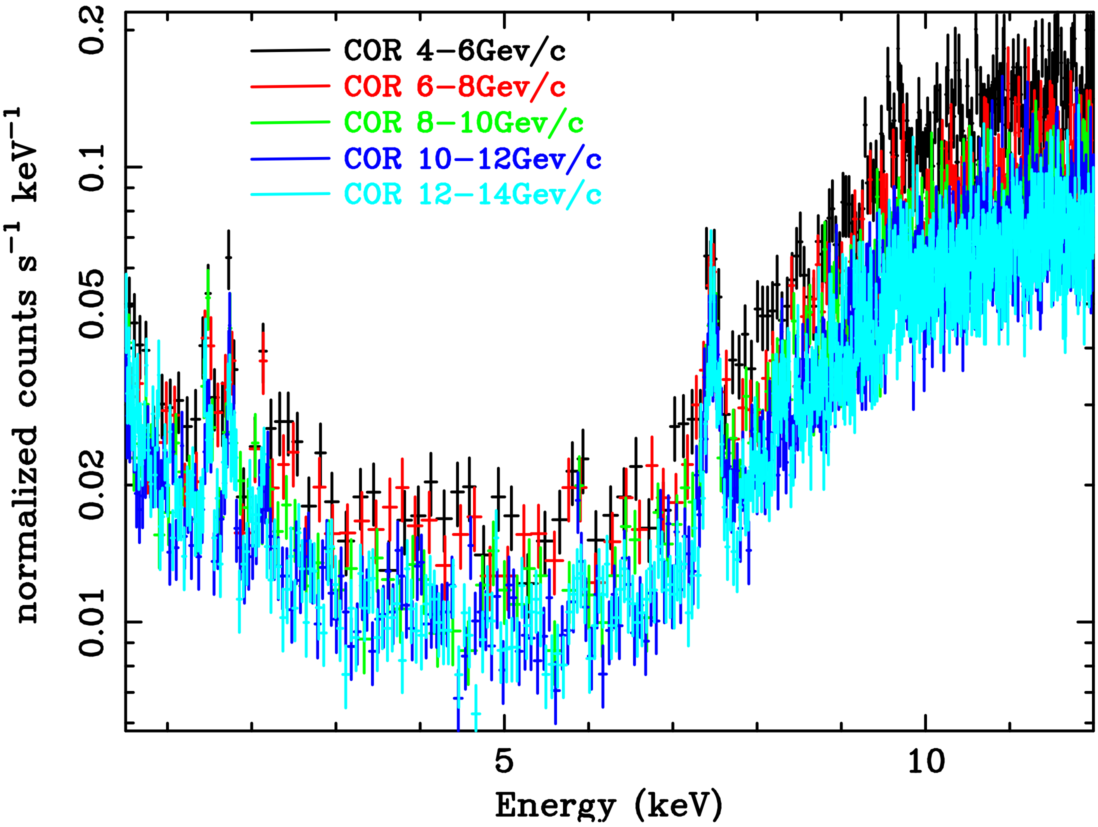

Figure 4: Internal background spectra of XIS1 taken from the different COR region.

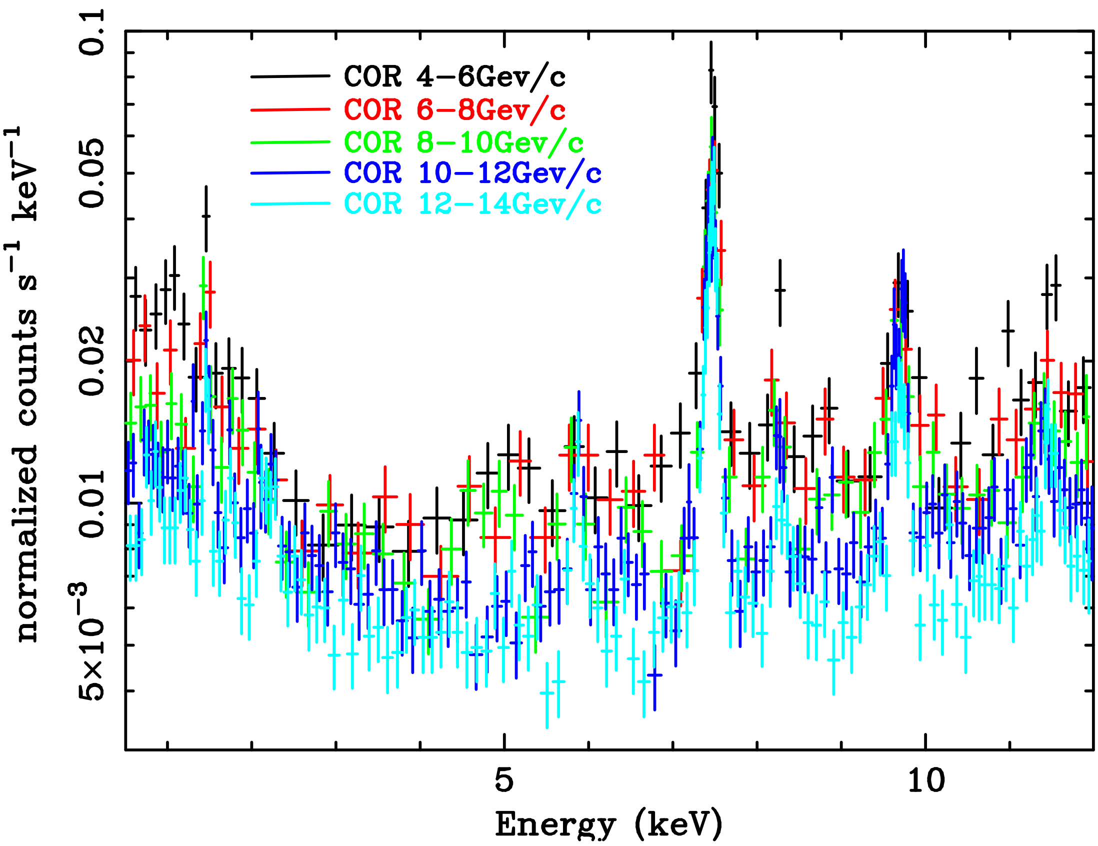

Figure 5: Internal background spectra of XIS2taken from the different COR region.

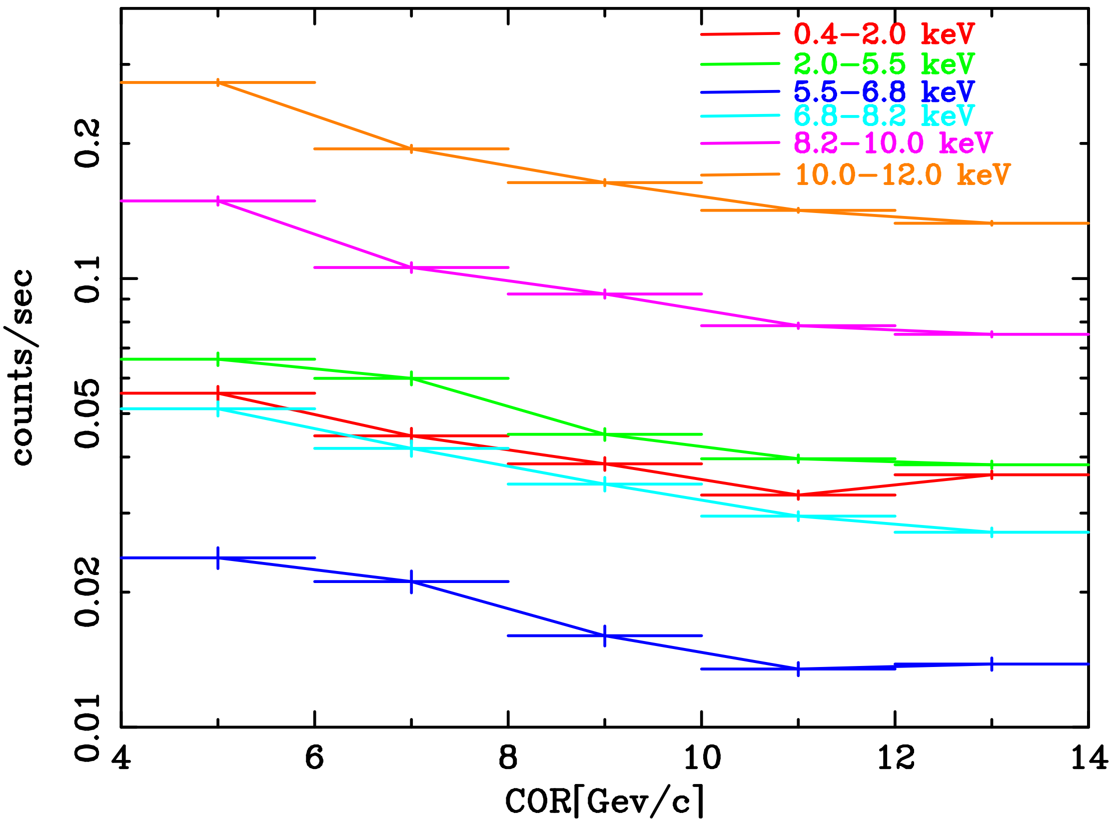

Figure 6: Count rate for different energy bands as a function of COR (XIS1).

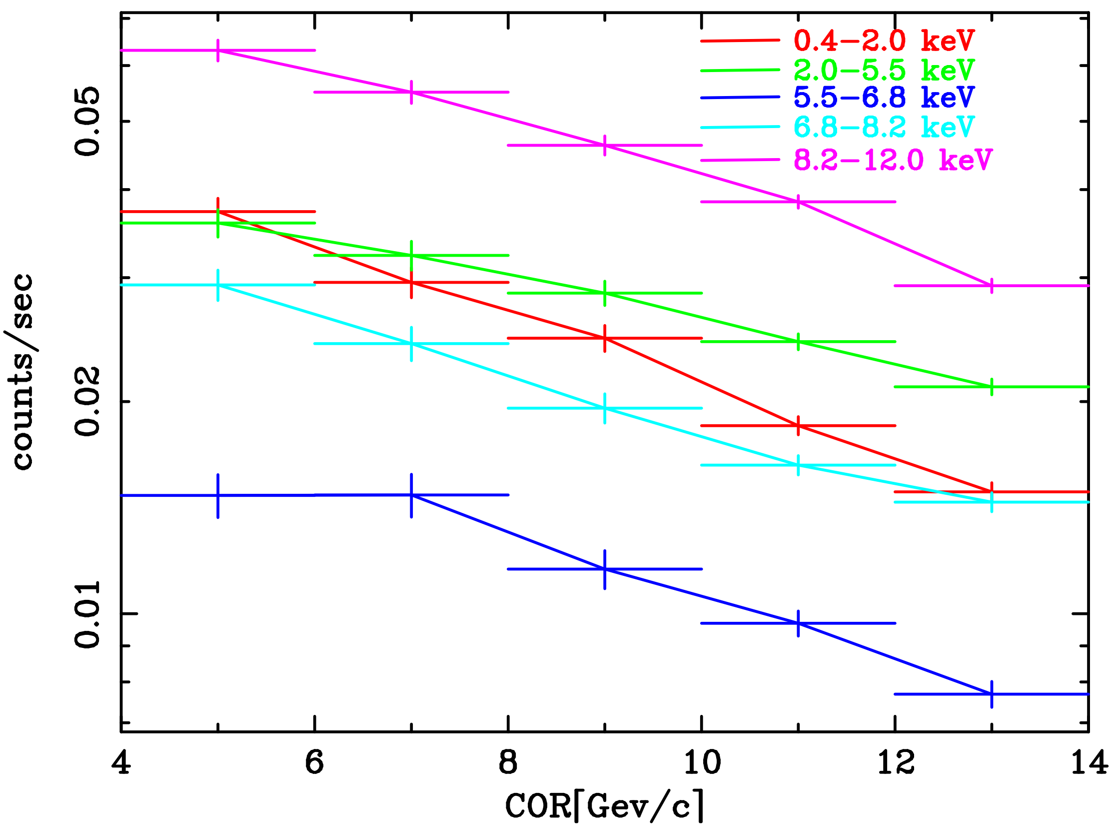

Figure 7: Count rate for different energy bands as a function of COR (XIS2).

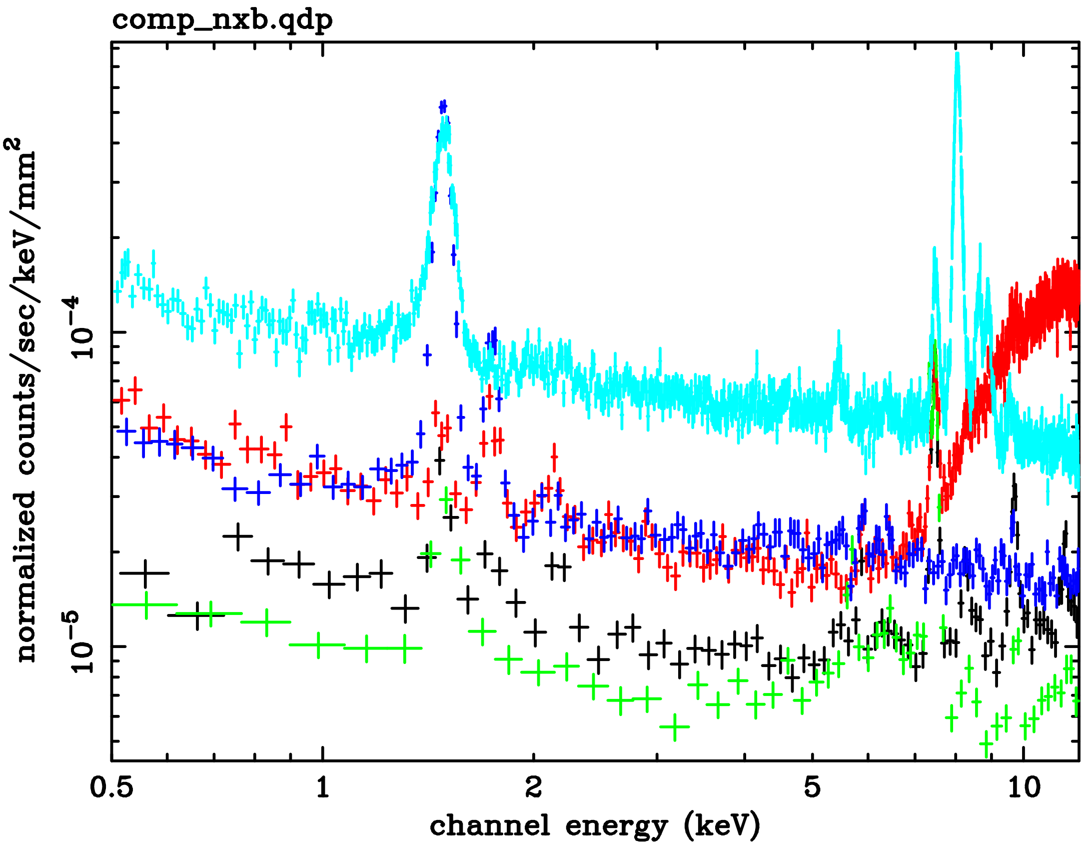

Figure 8: Internal background spectra of ASCA/SIS (green), Suzaku/XIS-FI (black), Suzaku/XIS-BI (red), XMM-Newton/PN (light blue), XMM-Newton/MOS(blue). Each spectra is normalized by the CCD area.

1.4 Comparison of the internal background

In figure 8, we compare the internal background spectra of ASCA/SIS, Suzaku/XISs, and XMM-Newton/PN, XMM-Newton/MOS. The spectra of ASCA/SIS and Suzaku/XISs are the night earth observation. The spectra of XMM-Newton are "CLOSED" data which taken with the filter wheel in the closed position. Each spectrum is normalized by the physical size of the CCD.

The background level of XIS-FI is similar to ASCA/SIS. The background level of XIS-BI is similar to XMM/MOS though it is gradually increase above 7 keV. The steep rise in background above 7 keV in the BI chip is related to its thickness (or thinness.) The BI chip is only about 45 μm thick. The FI chips are much thicker: they have depletion regions that are 60-75 μm thick, and undepleted substrates that are several hundred μm thick. So a given ionizing particle will generally deposit less total charge in the BI than in the FI. The larger amplitude in the FI chip makes it more likely the particle event can be distinguished from an X-ray by the event selection algorithm.

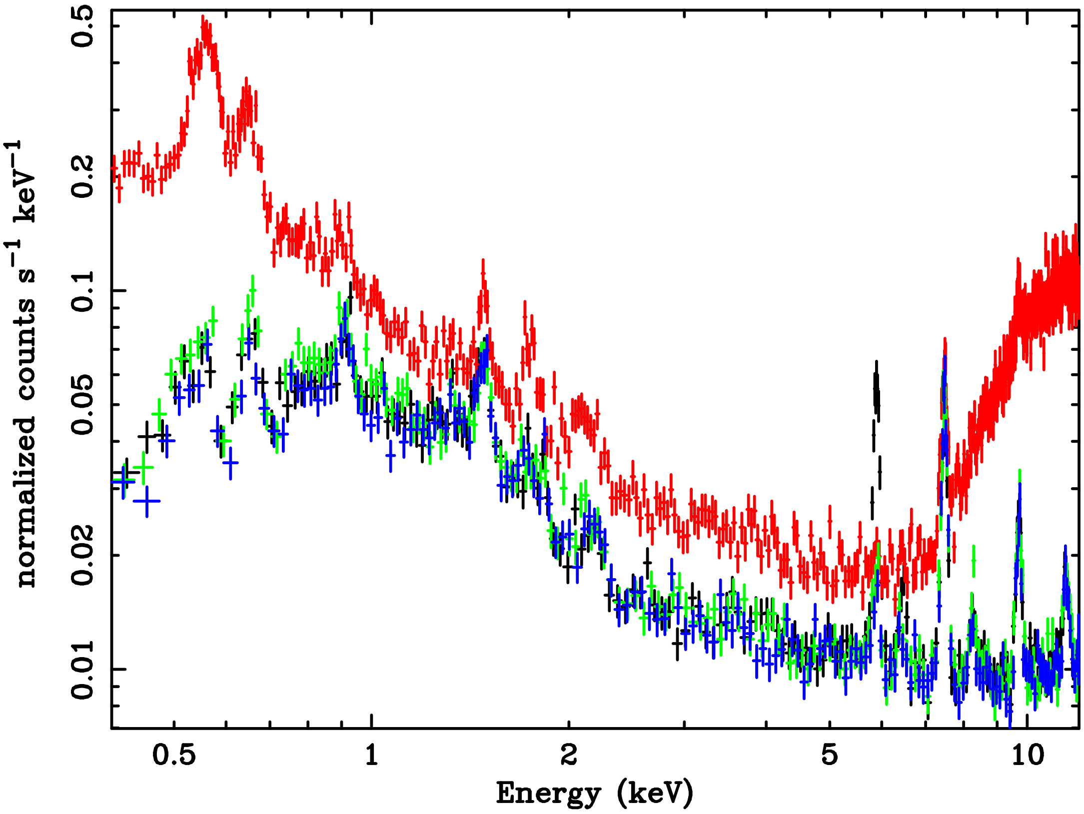

Figure 9: Comparison of the background of four XISs. XIS0 (black), XIS1 (red), XIS2 (blue), and XIS3 (green).

2 Sky background

In this section, we show the background spectrum which included cosmic X-ray background (CXB). The data was taken from the observation of North Ecliptic Pole (rev0.3 data, 109 ks)[2]. We extracted the background excluding the cal source region. Figure 9 shows the background spectrum of four XISs.

2.1 NXB and CXB

Figure 10 and 11 shows the comparison of the background of the NEP observation and the internal background (night earth observation). The internal background is dominant above 7 keV.

2.2 Comparison of the background

In this subsection, we compare the background of Suzaku/XIS-FI, Suzaku/XIS-BI, ASCA/SIS, XMM-Newton/MOS, XMM-Newton/PN, Chandra/ACIS-S, and Chandra/ACIS-I. The data of XMM-Newton and Chandra are the same in Katayama et al. (2004)[2].

Figure 12 shows the background spectra normalized by the physical size of the CCD. As these spectra include the CXB component, a direct comparison of the background is meaningful only above 5 keV (see also Figure 8).

Figure 13 shows the background spectra normalized by the effective area and by the solid angle of the FOV. Thus, it represents a surface brightness of the background, and gives a measure of S/N ratio to diffuse objects. An overlap of the curve in lower energy range[3] indicates that the CXB background is dominant at this energy range. For reference, we plot the CXB spectrum

$$I(E) = 9.3 \times 10^{-7} E^{-1.4} \quad [\mathrm{keV/cm^2/sec/keV/arcmin^2}] \tag{1}$$

in the same figure.

This plot demonstrates that Suzaku/XIS-FI (and ASCA/SIS) have a higher S/N ratio for diffuse objects than other instruments. At 7 keV, the S/N ratio of Suzaku/XIS-FI is 2–4 times higher than that of XMM-Newton.

[2]In the previous report, we used an early phase data of MCG 6-30-15. As this data was processed by the calibration data before launch, the results are slightly different from especially for the XIS-BI.

[3]There is a little scatter even in the lower energy range. This may be due to our procedure to make this plot, e.g., the value of the effective area is represented with that of the aim point.

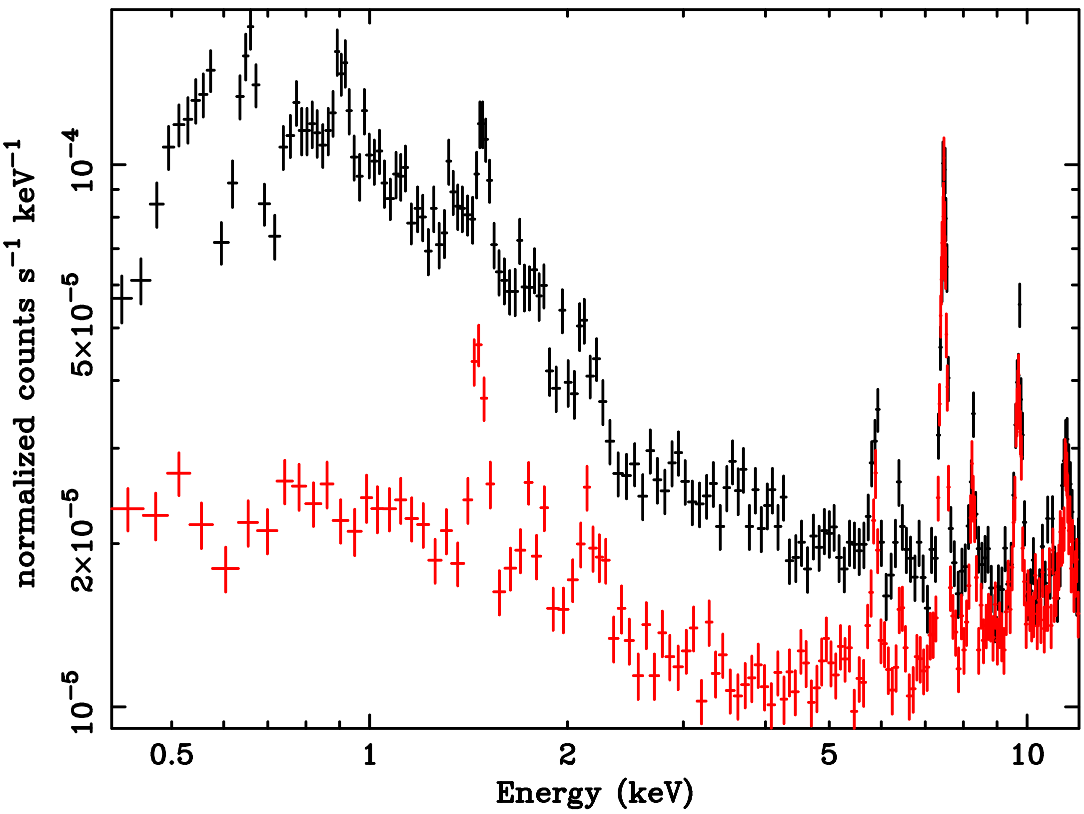

Figure 10: Comparison of the CXB (black) and the internal background (red) in the XIS-FI (XIS2) spectrum.

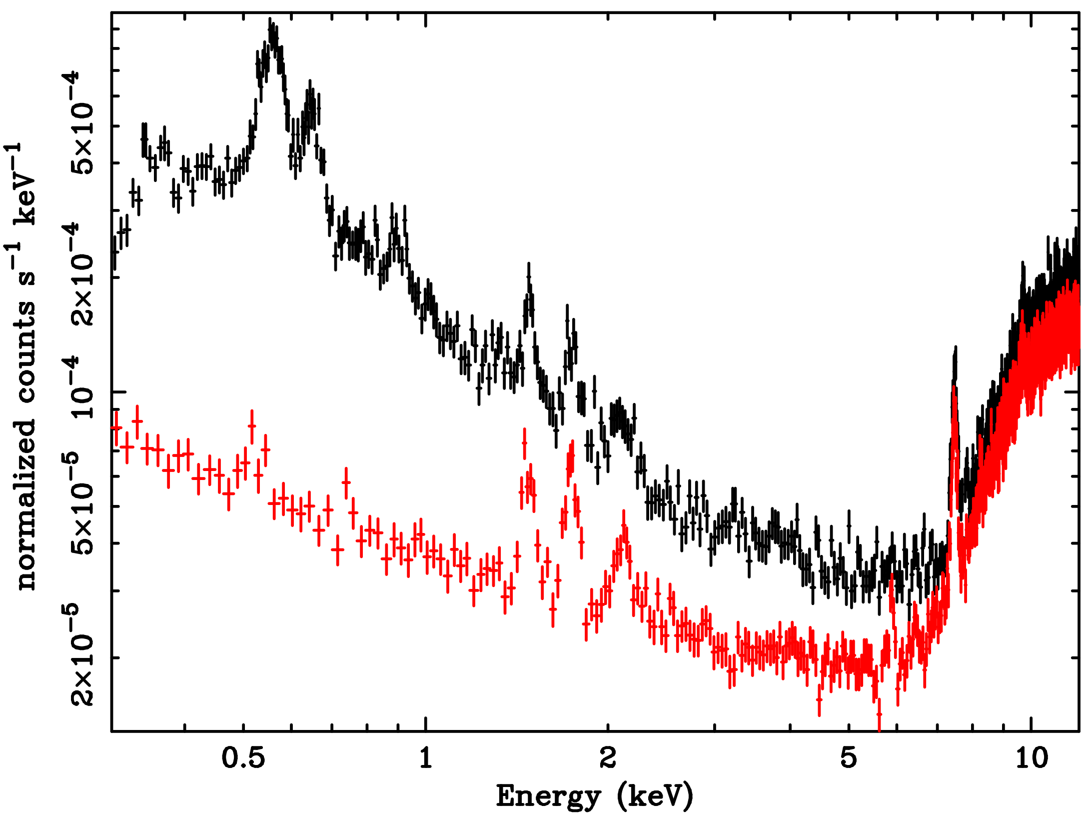

Figure 11: Comparison of the CXB (black) and the internal background (red) in the XIS-BI (XIS1) spectrum.

In other words, non X-ray background level in square arc minutes is dominant above 5 keV for Suzaku/XIS-FI, while the threshold is about 2 keV for XMM-Newton and 1 keV for Chandra.

Note that the sensitivity to the diffuse objects is not determined only by this S/N ratio. The temporal variation of the background and the uncertainty in a background model will also determine the sensitivity. We are going to examine the temporal variation of the XIS background and its relation to orbital and other parameters, in order to establish accurate background model.

References

[1] Gendreau, K., 1995, Ph.D. thesis, MIT

[2] Katayama, H., Takahashi, I., Ikebe, Y., et al., 2004, A&A 414, 767

[3] Yamaguchi, H., 2005, "Suzaku XIS background", internal report

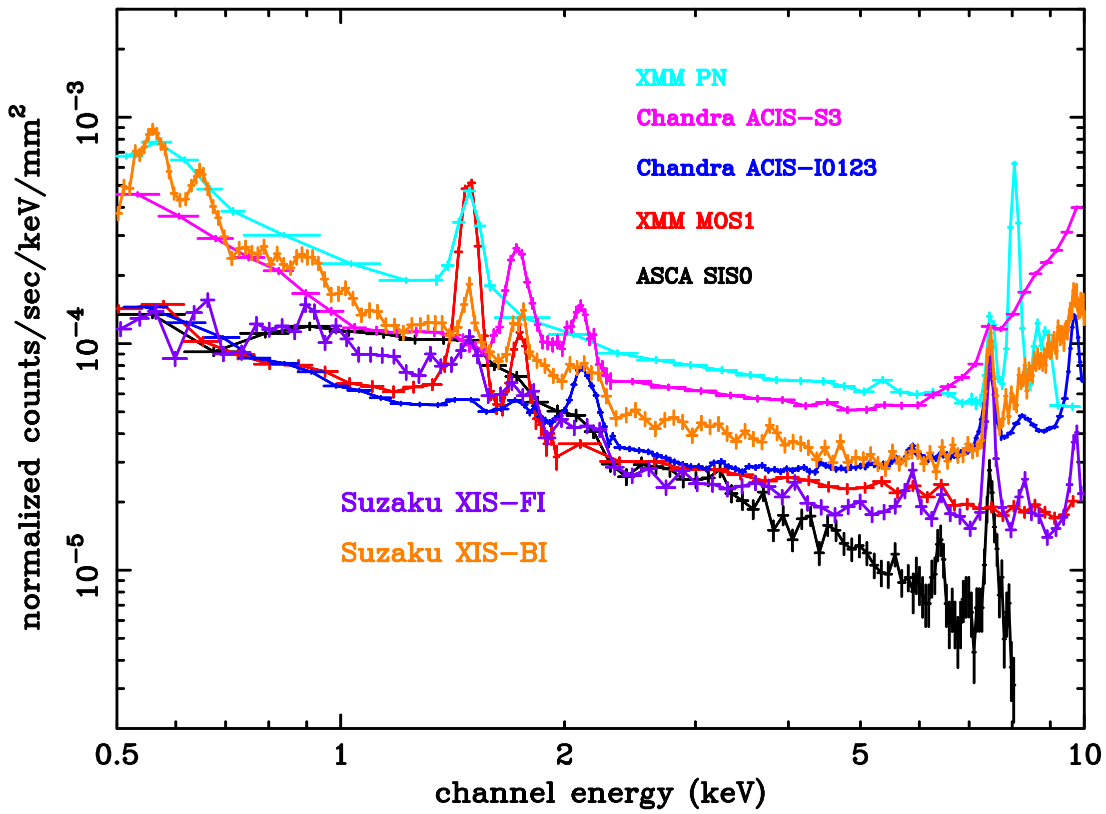

Figure 12: Comparison of the background spectra normalized by the physical size of the CCD.

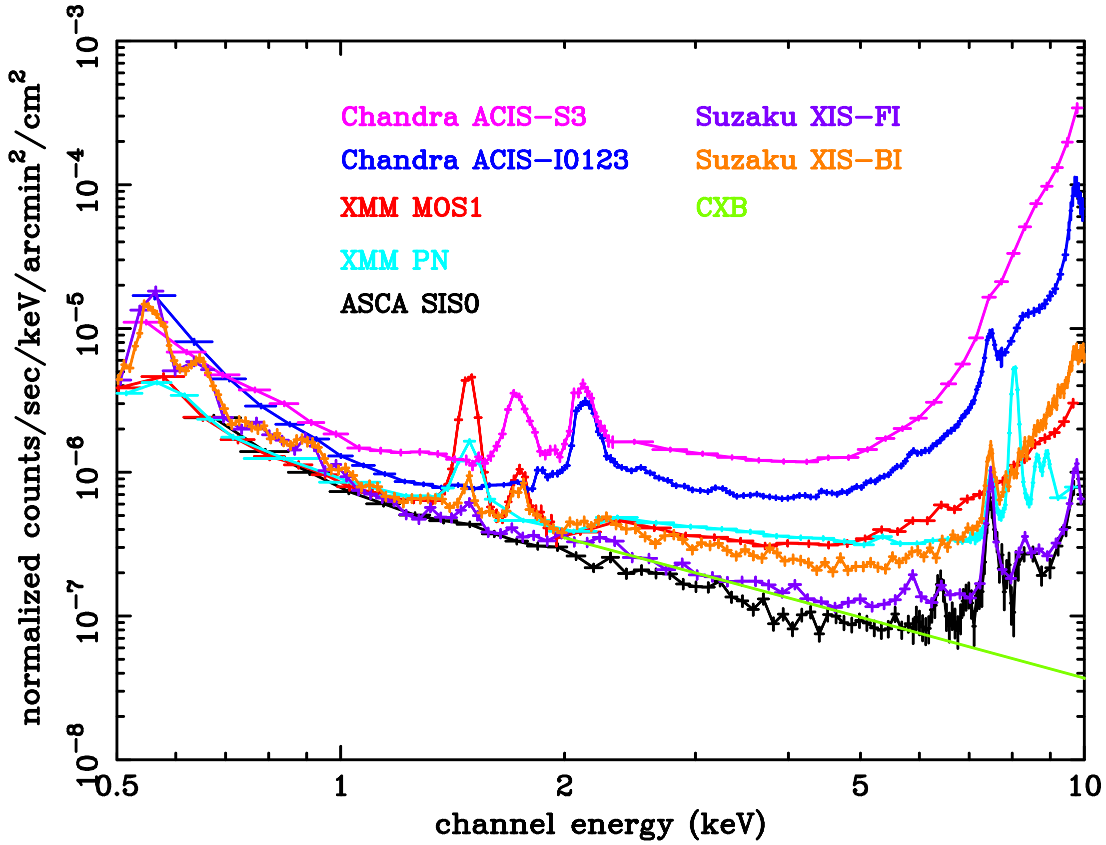

Figure 13: Comparison of the background spectra normalized by the effective area and by the FOV.